Synthesis and Characterization of PbS Nanocrystallites in Random Copolymer Ionomers

Zhaohua Zeng, Suhua Wang, and Shihe Yang*

Department of Chemistry, Hong Kong University of Science and Technology, Clear Water Bay, Kowloon, Hong Kong

Received July 8, 1999

Poly(methyl methacrylate-*co*-methacrylic acid) lead(II) salt ionomer [P(MMA-*co*-MAA)−Pb^{II}] has been prepared by the exchange reaction of poly(methyl methacrylate-*co*-methacrylic acid) with lead(II) acetate. PbS nanoparticles were synthesized by treating the [P(MMA-*co*-MAA)−Pb^{II}] powder with H_2S. The average PbS particle size was estimated to be ∼1−10 nm, depending on the preparation conditions. The particle size was found to increase with the increasing concentration of the carboxylic−lead(II) salt group content. Fourier transform infrared, UV−vis, X-ray diffraction, transmission electron microscopy, and differential scanning calorimetry techniques were employed to study the size, interfacial structure, and thermal properties of the PbS nanocrystals in the copolymer matrix.

Introduction

Lead sulfide, PbS, is a narrow band gap semiconductor. The absorption edge of PbS exhibits a large blue shift when one shrinks the crystallite size to the nanometer size regime.[1−7] It is expected that lead sulfide nanoclusters display greatly enhanced nonlinear optical properties compared with their bulk counterparts and have potential applications in optoelectronic devices.[8,9] Many methods have been developed to fabricate PbS nanoparticles in micelles,[10] polymers,[11] zeolites,[12] and monolayer surfaces.[13] The polymers used for synthesizing metal and semiconductor nanoparticles are normally amphiphilic block copolymers.[14] The hydrophilic micelles in amphiphilic block copolymers act as microreactors, where nanoparticles grow. The size and shape of the nanoparticles thus formed are largely determined by the corresponding properties of the micelles. A major challenge in adopting this method is to design and synthesize suitable amphiphilic block copolymers for nanoparticle templates.

The ready availability of ionomers makes them attractive as a template for the synthesis of semiconductor nanoparticles. The morphologies of ionomers have been widely studied in recent years.[15] It was found that ionic groups in ionomer macromolecules can gather together to form ionic domains, which are as small as a few nanometers in size and are phase separated from the polymer matrix. These ionic domains could be ideal nanoreactors for the semiconductor nanoparticle synthesis. Wang et al. first synthesized PbS nanoparticles in ionomers.[16] They characterized the structural, morphological, and optical properties of the PbS quantum dots and proposed theoretical models for the band structure dependence of PbS on its crystallite size. Although this work has opened a convenient avenue for synthesizing semiconductor nanoparticles, virtually no further work has followed along this line. Recently, we attempted to use random ionomers to prepare PbS semicondutor nanoparticles. We first prepared metal ion-containing ionomer as a precursor and then used gas−solid reactions to form the final well-dispersed semiconductor nanoparticles in the ionomer. In this paper, we report on the formation of lead sulfide semiconductor nanoparticles in poly(methyl methacetate-*co*-methylactic acid) [p(MMA-*co*-MAA)]. These nanoparticles/polymer hybrids were characterized with Fourier transform infrared (FITR), UV−vis spectra, X-ray diffraction (XRD), transmission electron microscopy (TEM), and differential scanning calorimetry (DSC). Furthermore, the effects of heat treatment on the particle size were studied in detail, and useful information about the nanoparticle growth mechanism was obtained.

Experiment

(1) Preparation of Poly(methyl methacrylate-*co*-methacrylic acid) Lead(II) Salt Ionomers [P(MMA-*co*-MAA)−

(1) Krauss, T. D.; Wise, F. W. *Phys. Rev. B* **1997**, *55*, 9860.
(2) Kang, I.; Wise, F. W. *J. Opt. Soc. Am. B* **1997**, *14*, 1632.
(3) Ogawa, S.; Hu, K.; Fan, F. R.; Bard, J. A. *J. Phys. Chem. B* **1997**, *101*, 5707.
(4) Nenadovic, M. T.; Comor, M. I.; Vasic, V.; Micic, O. I. *J. Phys. Chem.* **1990**, *94*, 6390.
(5) Machol, J. L.; Wise. F. W.; Patel, R.; Tanner, D. B. *Physica A* **1994**, *207*, 427.
(6) Zhou, H. S.; Sarahara, H.; Honma, I,; Komiyama, H. *Chem. Mater.* **1994**, *6*, 1534.
(7) Meldrum, F. C.; Flath, J.; Knoll, W. *Langmuir* **1997**, *13*, 2033.
(8) Banyai, L.; Hu, Y. Z.; Lindberg, M.; Koch, S. W. *Phys. Rev. B* **1988**, *38*, 8142.
(9) Olshavsky, M. A.; Goldstein, A. N.; Alivisatos, A. P. *J. Am. Chem. Soc.* **1990**, *112*, 9438.
(10) Eastoe, J.; Cox, R. A. *Colloids Surfaces A* **1995**, *101*, 63.
(11) Kane, R. S.; Cohen, R. E.; Silbey, R. *Chem. Mater.* **1996**, *8*, 1919.
(12) Mukherjee, M.; Datta, A.; Chakravorty, D. *Appl. Phys. Lett.* **1994**, *64*, 1159.
(13) Zhao, X. K.; Xu, S. Q.; Fendler, J. H. *Langmuir* **1991**, *7*, 520.
(14) Forster, S.; Antonietti, M. *Adv. Mater.* **1998**, *10* (3), 195.
(15) Eisenberg, A.; Kim, J.-S. *Introduction to Ionomers*; John Wiley & Sons: New York, 1998.
(16) Wang, Y.; Suna, A.; Mahler, W.; Kasowski, R. *J. Chem. Phys.* **1987**, *87*, 7315.

10.1021/cm990425o CCC: $18.00 © 1999 American Chemical Society
Published on Web 10/27/1999

Pb^{II}]. Three polymer solutions were prepared by dissolving 10 g of P(MMA-*co*-MAA) (Aldrich, average M_n ~15 000) in 100 mL of chloroform. The molar ratio of MMA to MAA in the copolymer is 100:16. Different amounts of a methanol solution containing 0.25 M lead(II) acetate were added into each of the above polymer solutions. The resulting three solutions with the Pb(II) mole fractions of 5.0, 2.5, and 1.0%, respectively, were refluxed for 2 h at 1 atm to ensure the completeness of the ion exchange reaction. After solvent evaporation at room temperature, the precipitates were stored in a vacuum oven at 70 °C for 12 h to remove the residual acetic acid. Finally, white solid samples of the P(MMA-*co*-MAA)−Pb^{II} ionomers with different lead(II) loading were obtained, and they were pestled to a powder in an agate mortar.

(2) Formation of PbS Nanoparticles. PbS nanoclusters can be prepared by treating the ionomers with H_2S either in a solution or in the solid state. By using a very dilute lead(II)−ionomer solution (<10^{-3} M), we had prepared a stable solution of PbS in $CHCl_3$. However, the size of the PbS particles obtained in the solution was too small (~1 nm as judged from the UV−vis spectrum), and no diffraction peaks could be observed in the XRD profile. As the concentration of the Pb(II) ionomer solution was increased, PbS precipitated rapidly upon H_2S treatment, and the precipitate could not be redissolved. Therefore, it is difficult to obtain stable PbS nanoparticle solution with a tunable PbS nanoparticle size by using the solution treatment method. We then proceeded with the solid-state treatment method.

Considering that a suitable lead(II)−ionomer film for H_2S treatment is difficult to prepare, we used fine powder samples of the lead(II)−ionomers to synthesize PbS nanoparticles. Fine powders of P(MMA-*co*-MAA)−Pb^{II} ionomers with various amounts of lead(II) were treated with hydrogen sulfide overnight. After the hydrogen sulfide treatment, the sample changed color from light yellow to dark brown, depending on the quantity of lead(II) loaded into the ionomers. The resulting PbS/ionomer nanocomposites could be dissolved in $CHCl_3$, forming a stable solution.

(3) Characterization. Perkin-Elmer 16PC FTIR spectrometer was used for FTIR measurements. UV−vis spectra were obtained with a Milton Roy 3000 array spectrophotometer. The solution for UV−vis measurement was prepared by dissolving the P(MMA-*co*-MAA)−PbS powder in $CHCl_3$. Powder X-ray diffraction (XRD) measurements were carried out in a Philips PW1830 instrument with a 1.54 Å Cu Kα rotating anode point source. The source was operated at 40 kV and 40 mA, and the Kβ radiation was eliminated using a nickel filter. TEM experiments were performed with a Joel 100 instrument, at an operating voltage of 100 kV. Setaram Model DSC92 was used for the DSC measurements. All samples with different lead loading were treated under identical conditions prior to all the characterization experiments.

Results and Discussion

(1) Formation of PbS Nanoparticles. Figure 1 shows an XRD pattern of the PbS nanocrystals dispersed in P(MMA-*co*-MAA) with the PbS mole fraction of 5%. The diffraction peaks have a one-to-one correspondence to those of the cubic rock-salt structure of bulk PbS. The average diameter of the PbS nanoparticles was calculated on the basis of the Scherer's equation, $D = k\lambda/(\beta\cos\theta)$, where β is the half-width of the diffraction peak, λ is the X-ray wavelength (1.542 Å), and k is a geometric factor (0.89). We estimated the average PbS particle size to be 7.8 nm. The corresponding TEM image of these PbS nanocrystals are presented in Figure 2. Overall, the polymer-capped PbS nanoparticles are roughly spherical in shape and are well-separated from each other. The nanoparticle diameter distribution is shown in Figure 3. The PbS particle size is relatively uniform. The average diameter of the PbS particles is estimated to be ~8.7 nm on the basis of the analysis of the TEM images (the number average $\langle d\rangle = \sum n_i d_i/\sum n_i$), which is in fairly good agreement with that obtained from the XRD measurement.

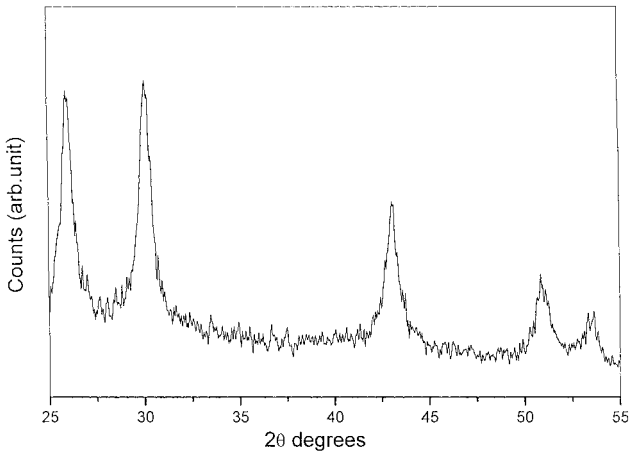

Figure 1. XRD profile of the as synthesized P(MMA-*co*-MAA)−PbS with the mole fraction of PbS being 5.0%.

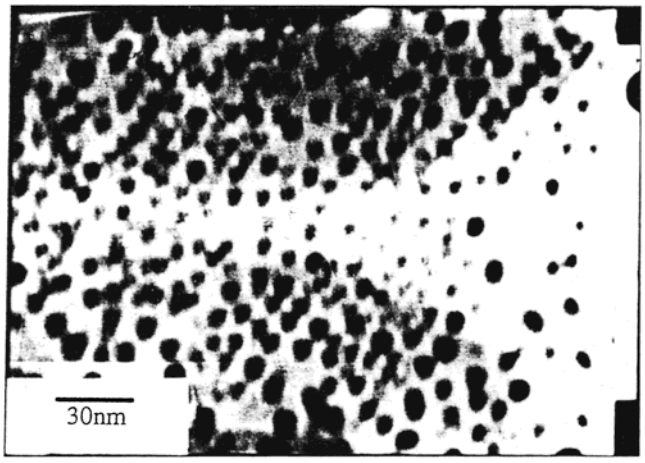

Figure 2. TEM micrograph of the as synthesized P(MMA-*co*-MAA)−PbS with the mole fraction of PbS being 5.0%.

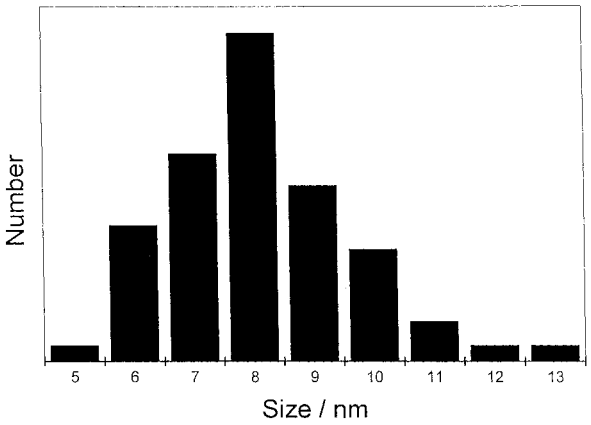

Figure 3. Histogram showing the diameter distribution of the as synthesized PbS nanoparticles based on the TEM micrograph such as that shown in Figure 2.

Plotted in Figure 4 are FTIR spectra of the copolymer with and without the loading of Pb(II) or PbS. A new absorption peak at 1560 cm^{-1} shows up when the copolymer is loaded with Pb(II). This peak can be attributed to the formation of carboxylic lead(II) groups in P(MMA-*co*-MAA)−Pb^{II} (curve 2). The peak disappears

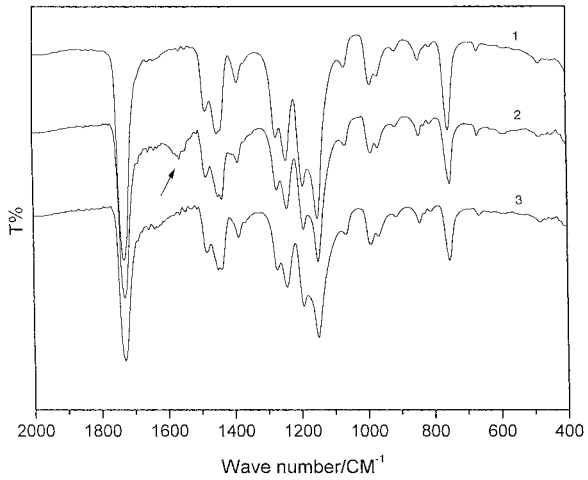

Figure 4. FTIR transmission spectra of P(MMA-*co*-MAA) (curve 1), P(AAM-*co*-MAA)−Pb^{II} (curve 2), and P(MMA-*co*-MAA)−PbS (curve 3). The Pb(II) mole fraction is 5.0%.

Table 1. Average Diameters (d)[a] of the PbS Nanoparticles Formed in P(MMA-*co*-MAA) As Estimated from the XRD Data

samples	PbS in polymer (mol %)	d_0 (nm)	d_1 (nm)	d_2 (nm)
P(MMA-*co*-MAA)−PbS-1	5.0	7.8	7.6	11.5
P(MMA-*co*-MAA)−PbS-2	2.5	5.3	5.2	10.6
P(MMA-*co*-MAA)−PbS-3	1.0	1.8	1.9	3.3

[a] d_0 is for the original powder samples; d_1 is for the samples after heat treatment under a vacuum oven at 100 °C for 5 h, and d_2 at 140 °C for 5 h.

after the sample is treated with hydrogen sulfide (H_2S). Presumably, when the ionomer was treated with H_2S, PbS was formed, and the salt groups were changed to the carboxylic acid groups. In other words, the polymer chains were changed back to the original carboxylic acid structure after H_2S treatment. As is evident in Figure 4, the sample of P(MMA-*co*-MAA)−Pb^{II} which has been treated with hydrogen sulfide for 10 h has the same IR spectrum as that of the original polymer P(MMA-*co*-MAA). This indicates that the carboxylic groups were recovered in the ionic domains after the H_2S treatment.

(2) Effect of the Ionic Group Pb(II) Content on the PbS Nanoparticle Size. For the ionomer samples with a different loading of Pb(II), we estimated the PbS nanoparticle size by examining the width of the X-ray diffraction peaks. As mentioned above, we estimated the average diameter of the PbS nanoparticles using the Scherer's equation for the PbS/ionomer composites containing different mole fractions of Pb(II). The results are listed in Table 1. It can be seen that the size of the PbS nanoparticles increases with the increasing content of the ionic groups Pb(II).

Figure 5 presents the UV−vis absorption spectra of P(MMA-*co*-MAA)−PbS samples in $CHCl_3$ with different contents of PbS by plotting $(\alpha h\nu)^2$ vs $h\nu$, where α is the absorption coefficient and $h\nu$ is the photon energy. In this way, direct band gaps E_g of PbS nanoclusters can be determined by extrapolation based on the relation $\alpha h\nu = A(h\nu - E_g)^{1/2}$. It should be mentioned that the absorption coefficients α were normalized to the volume concentrations of PbS, which were taken to be the initial concentrations of Pb(II). For the UV−vis absorption measurements, we deliberately prepared the samples

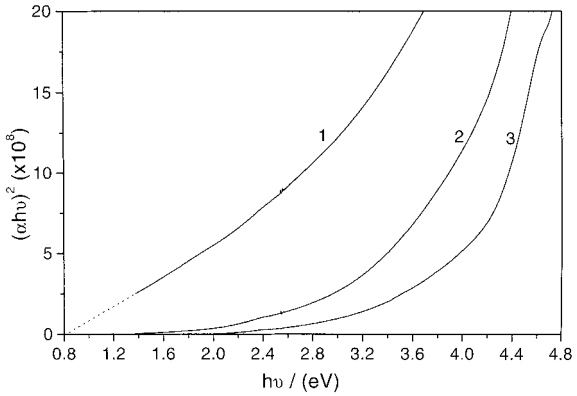

Figure 5. UV−vis absorption spectra of P(MMA-*co*-MAA)−PbS in $CHCl_3$ with the mole fractions of PbS being (1) 5.0, (2) 2.5, and (3) 1.0%.

Table 2. Band Gaps and Estimated Diameters of the PbS Nanoparticles from the UV−vis Spectra

samples	band gap (eV)	band gap wavelength (nm)	d(nm)
P(MMA-*co*-MAA)−PbS-1	0.84	1430	7.3
P(MMA-*co*-MAA)−PbS-2	1.27	1000	4.5
P(MMA-*co*-MAA)−PbS-3	2.03	600	2.7

Table 3. DSC Results (Glass Transition Temperature, T_g) for the Salts P(MMA-*co*-MAA)−Pb^{II} before and after H_2S Treatment

samples	Pb(II) in polymer (%)	T_g (°C)
Before H_2S treatment		
P(MMA-*co*-MAA)Pb-1	5.0	123.3
P(MMA-*co*-MAA)Pb-2	2.5	123.0
P(MMA-*co*-MAA)Pb-3	1.0	121.9
After H_2S treatment		
P(MMA-*co*-MAA)/PbS-1	5.0	122.2
P(MMA-*co*-MAA)/PbS-2	2.5	123.2
P(MMA-*co*-MAA)/PbS-3	1.0	121.1
P(MMA-*co*-MAA)	0	118.6

of similar PbS volume concentrations in $CHCl_3$ so as to minimize the concentration effect of PbS on the band gap estimation. Briefly, 10, 6, and 3 mg of the samples P(MMA-*co*-MAA)−PbS-3, -2, and -1 were dissolved in 10 mL of chloroform, respectively. The corresponding concentrations of PbS for the above three solutions were calculated to be 1.96×10^{-4} M, 2.38×10^{-4} and 2.40×10^{-4}, respectively.

As seen from Figure 5, dramatic blue shifts of the absorption edge show up for the polymer-protected PbS nanoparticles compared with the bulk band gap of PbS (0.41 eV). The blue shifts of the absorption edge increases as the Pb(II) content decreases (Table 2), indicating a decrease in the PbS nanoparticle size. The diameter of the PbS nanoparticles was also estimated on the basis of the hyperbolic model using the band gap value obtained from the UV−vis absorption edge (see Table 2).[1] The result is in reasonable agreement with that obtained from the XRD measurements. The exciton absorption peaks of the PbS nanoparticles at 600 nm did not appear in the UV−vis spectra, presumably because the surface of the PbS nanoparticles were at least partially capped by the carboxylic acid groups.

(3) Thermal Properties of the PbS/Ionomer Composites. Table 3 lists the measured glass transition temperatures (T_g) of P(MMA-*co*-MAA)−Pb^{II} ionomers with different concentrations of Pb(II) before and after

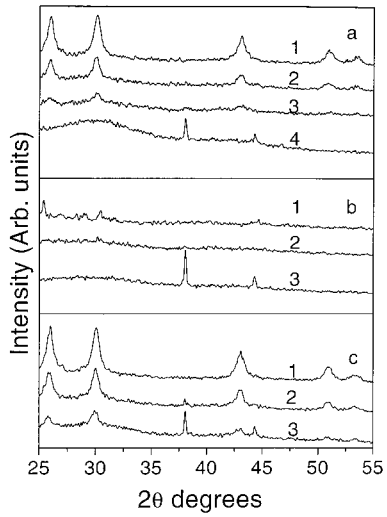

Figure 6. XRD patterns of (a) the as synthesized P(MMA-*co*-MAA)−PbS with different mole fractions of PbS, (b) the as synthesized P(MMA-*co*-MAA)−Pb^{II} with different mole fractions of Pb(II), and (c) P(MMA-*co*-MAA)−PbS with different mole fractions of PbS after heat treatment under a vacuum at 100 °C for 5 h. The mole fractions of PbS or Pb(II) are (1) 5.0, (2) 2.5, (3) 1.0, and (4) 0%.

the H_2S treatment. The data were obtained on the basis of the DSC measurements at 10 K/min. The T_g of Pb(II)-loaded ionomers is in general 3−5 °C higher than that of the pure copolymer P(MMA-*co*-MAA). The increase in T_g for the Pb(II)-loaded ionomers is apparently due to the more restricted motion of the macromolecular chains after the aggregation of ionic groups and therefore the formation of clusters. It was also found that the T_g's of H_2S-treated P(MMA-*co*-MAA)−Pb^{II} ionomers do not exhibit a distinguishable decrease compared with the P(MMA-*co*-MAA)−Pb^{II} ionomers without H_2S treatment. It is therefore reasonable to expect that there are still interactions between newborn PbS nanoparticles and the carboxylic groups in the ionomers, which hinder the motion of the macromolecular chains.

We have studied the effect of heat treatment on the copolymer structures in the PbS/ionomer composite. Figure 6 shows a series of XRD profiles of P(MMA-*co*-MAA), P(MMA-*co*-MAA)−Pb^{II}, and P(MMA-*co*-MAA)−PbS samples. For the pure copolymer sample P(MMA-*co*-MAA), there are one broad bump at $2\theta = 30°$ and two sharp diffraction peaks at $2\theta = 38.0$ and 44.2° (Figure 6a, curve 4). The broad bump is due to the amorphous phase of the polymer, and the two sharp diffraction peaks can be attributed to the microcrystalline domains of the polymer chains. In the P(MMA-*co*-MAA)−PbS system, however, these two peaks disappear, and only the diffraction peaks due to the PbS cubic rock-salt structure are observed (see Figure 6a, curves 1−3). This indicates that the formation of PbS nanoparticles disturbed the ordered arrangement of the molecular chains. More importantly, this also implies that the PbS nanoparticles are highly dispersed in the polymer matrix without forming phase-segregated extended polymer and PbS domains. A similar phenomenon was observed for the P(MMA-*co*-MAA)−Pb^{II} salt ionomers with a high content of the salt groups (Figure 6b, curves 1 and 2): the diffraction peaks at 38.0 and 44.2° disappeared for a sufficiently high concentration of Pb(II). In this case, we believe that it is the ionic aggregates that affect the arrangement of molecular chains, preventing them from crystallization.

After heat treatment of the P(MMA-*co*-MAA)−PbS system under a vacuum at 100 °C for 5 h, the two sharp diffraction peaks at 38.0 and 44.2° reappeared in addition to those due to the cubic rock-salt structure of PbS at the lowest Pb(II) concentration (Figure 6c, curve 3). The relative intensities of the two sharp diffraction peaks decreased when the Pb(II) concentration decreased (Figure 6c, curve 2). No diffraction peaks at either 38.0 or 44.2° were observed at the highest Pb(II) concentration (Figure 6c, curve 1). This demonstrates that the copolymer chains tend to recrystallize at a relatively low Pb(II) concentration at this temperature, which is understandable because the ionic Pb(II) groups have a tendency to disrupt the polymer microcrystalline domains.

It should be pointed out that the heat treatment described above was carried out at a temperature of 100 °C, which was close but below the T_g (∼120 °C) of the copolymer. Although the copolymer phase structure changed significantly at this temperature, the size of the PbS nanoparticles remained essentially unchanged. This can be clearly seen in Table 1. However, when the heat treatment was carried out above the T_g of the copolymer, e.g., 140 °C, for the same length of time, significant increase in the size of the PbS nanocrystals was observed (see Table 1). This demonstrates that the PbS nanoparticles aggregated in the ionomer matrix, forming larger particles when annealed above the T_g of the ionomers, but they are quite stable when annealed below the T_g. At the lower temperature, only the local rearrangement of polymer chains is possible, and this may have changed the polymer phase structure, leading to the reappearance of the two diffraction peaks at 38.0 and 44.2°. When the heat treatment temperature is above the T_g of the copolymer, long-range movement of polymer chains is possible, which increases the diffusion rate of the PbS nanocrystals and facilitates their aggregation. Another interesting result from Table 1 is that small particles are more susceptible to aggregation compared with large particles when the annealing was carried out above the T_g of the ionomers. This is likely to be due to their higher diffusion rate in the polymer matrix.

There may be two mechanisms for the size increase of the PbS nanoparticles during the annealing processes. One is the coalescence of the nanoparticles. In this mechanism, one would expect that the number of the nanoparticles decreases as the size of the nanoparticles increases. Another mechanism involves the absorption of PbS molecules or small clusters by the PbS nanoparticles, i.e., Ostwald ripening. It is likely that the PbS molecules and small clusters spread out in the polymer matrix, and they may not have the chance for extensive aggregation at room temperature. The distinguishing feature of this mechanism is that the number of the PbS nanoparticles does not decrease as the particle size increases during the annealing process. The latter mechanism may be more plausible considering that the nanoparticles size was never really doubled after annealing, while the size-doubling is expected for the coalescence mechanism. When the annealing is carried out above the T_g of ionomers, the facile movement of

the polymer chains increases the diffusion rate of the PbS molecules and clusters. When these molecules and clusters encounter the PbS nanoparticles, Oswald ripening occurs, leading to the increase of the nanoparticle size.

Conclusion

We have shown that PbS nanoparticles can be prepared by treating the ionomer P(MMA-*co*-MAA)−Pb^{II} powder with H_2S. FTIR shows a new absorption peak at 1560 cm^{-1} attributable to the carboxylic lead(II) groups of P(MMA-*co*-MAA)−Pb^{II}. The peak disappeared after exposure of P(MMA-*co*-MAA)−Pb^{II} to H_2S, suggesting the breakage of the Pb−O bond during the course of PbS growth. The PbS nanocrystallites were characterized by UV−vis spectroscopy. Significant blue shifts in the UV−vis absorption edge were observed for the PbS nanoparticles dispersed in the ionomers in comparison with the bulk PbS. Moreover, the blue shifts decreased with the increasing concentration of the salt groups, indicating an increase of the PbS particle size. The average PbS particle size was estimated to be ∼1−10 nmr, depending on the preparation conditions. The particle size was found to increase with the increasing concentration of the carboxylic−lead(II) salt group content. The size of the particles can be controlled by changing the amount of ionic groups in the ionomer and by heat treatment above the T_g of the ionomer. It provides a convenient way to synthesize semiconductor nanoparticles in a polymer matrix. We anticipate that other types of nanoparticles, particularly the II−VI chalcogenide semiconductor nanoclusters, can also be prepared by changing the ionic groups in the ionomers.

Acknowledgment. This work was supported by an RGC grant administered by the UGC of Hong Kong.

CM990425O